

Solving the riddle of the intradiol and extradiol catechol dioxygenases: how do enzymes control hydroperoxide rearrangements?

Timothy D. H. Bugg* and Gang Lin

Department of Chemistry, University of Warwick, Coventry CV4 7AL

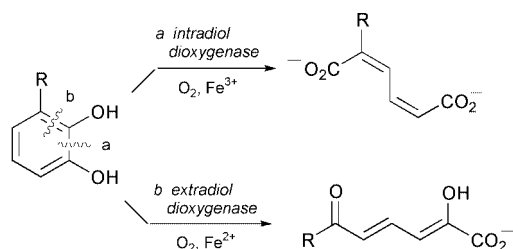
Received (in Cambridge, UK) 12th January 2001, Accepted 7th March 2001

First published as an Advance Article on the web 20th April 2001

Metallo-enzymes catalyse a rich variety of biochemical reactions, some of which have little or no precedent in laboratory chemistry.¹ Studies of such enzyme-catalysed reactions have benefited greatly in recent years from the pace of new protein X-ray crystallographic structures, but a detailed understanding of enzyme-catalysed reactions at the molecular level has required an interplay between structural studies, mechanistic studies, and small molecule model studies. This article will describe recent studies on an intriguing and long-standing puzzle in mechanistic enzymology, that of the non-haem iron-dependent catechol dioxygenases.²

Discovery of the catechol dioxygenases

A number of soil bacteria, especially *Pseudomonas*, have the metabolic capability to degrade aromatic compounds and utilise these compounds as the sole carbon source for growth.³ A key step in these catabolic pathways is the oxidative cleavage of catechol, or substituted catechols, to give acyclic products. Two families of dioxygenase enzyme were discovered by O. Hayaishi which can catalyse the oxidative cleavage of catechol, both families utilising dioxygen as a substrate (see Scheme 1).^{4–6} The intradiol dioxygenases, typified by catechol 1,2-diox-



Scheme 1 Reactions catalysed by intradiol and extradiol dioxygenases.

genase (or pyrocatechase), cleave the carbon–carbon bond between the phenolic hydroxy groups to yield muconic acid as product, and require Fe^{3+} as a cofactor.⁴ The extradiol dioxygenases, typified by catechol 2,3-dioxygenase (or meta-pyrocatechase), cleave the carbon–carbon bond adjacent to the phenolic hydroxy groups to yield 2-hydroxymuconaldehyde as product, and require Fe^{2+} as a cofactor.⁵

Unlike the cytochrome P450-dependent oxygenases, which were discovered at this time, the metal co-factors were utilised as non-haem iron by these enzymes. Hayaishi was able to demonstrate, using $^{18}\text{O}_2$ labelling experiments, that catechol 1,2-dioxygenase incorporated both atoms of oxygen from dioxygen into the reaction products,⁴ hence the designation as a dioxygenase. The mechanism invoked by Hayaishi to explain these results was that a four-membered dioxetane ring was formed during the reaction (see Scheme 2), which fragmented to form the reaction products.⁶

The reason for the different metal ion requirement of the two families of enzyme, however, remained a mystery. The intradiol

dioxygenases were entirely selective for Fe^{3+} , and were inactivated by treatment with reducing agents; while the extradiol dioxygenases were entirely selective for Fe^{2+} , and were inactivated by treatment with oxidising agents. Each family of enzyme was quite specific for the production of their respective reaction product with a range of substrates. Furthermore, although catechol is well known to be sensitive to aerial oxidation, oxidative cleavage of catechol was a reaction unprecedented in organic chemistry.

X-Ray crystallography of catechol dioxygenases

Although the catechol dioxygenases were demonstrated by Hayaishi to be crystalline enzymes,⁴ it was not until 1988 that the first X-ray structure of a catechol dioxygenase, the intradiol-cleaving protocatechuate 3,4-dioxygenase from *Pseudomonas putida*, was solved by Ohlendorf *et al.*⁷ The enzyme consists of two subunits, in an oligomeric $(\alpha\beta\text{Fe})_{12}$ structure (see Fig. 1B). The non-haem iron(III) cofactor was found to be ligated by four amino acid sidechains: the imidazole sidechains of His-460 and His-462, and the phenolic sidechains of Tyr-408 and Tyr-447 (see Fig. 1D). A fifth water ligand completes a trigonal bipyramidal structure. The two tyrosinate ligands are thought to stabilise the iron(III) cofactor and give the enzyme its characteristic deep red colour due to ligand-to-metal charge transfer interactions.⁷ X-ray structures of protocatechuate 3,4-dioxygenase from *Pseudomonas aeruginosa* and *Acinetobacter* sp. ADP1 have also been solved.^{8,9}

Recently another member of the intradiol dioxygenase family, catechol 1,2-dioxygenase from *Acinetobacter* sp. ADP1, has also been solved.¹⁰ This enzyme consists of an α_2 homodimer with one iron(III) cofactor per subunit. The tertiary structure of the 1,2-CTD enzyme is similar to that found in 3,4-PCD, although 1,2-CTD contains a novel helical zipper motif at the interface of the two subunits, and contains two molecules of bound phospholipid (see Fig. 1A). The active site of 1,2-CTD contains a very similar arrangement of iron(III) ligands: Tyr-200 and His-226 are the axial ligands, and Tyr-164, His-224 and a water molecule are the equatorial ligands (see Fig. 1C).¹⁰

Structural elucidation of the iron(II)-dependent extradiol dioxygenases has proved more challenging, due largely to the facile oxidation of the cofactor. By carrying out the enzyme purification and crystallisation under an anaerobic atmosphere, Han *et al.* were in 1996 able to solve the structure of 2,3-dihydroxybiphenyl 1,2-dioxygenase (BphC) from *Pseudomonas* LB400,¹¹ a strain capable of degrading chlorinated biphenyls. The tertiary structure of the enzyme consists of two similar $\beta\alpha\beta\beta$ domains, only one of which contains an iron(II) cofactor (see Fig. 2A). A funnel-shaped cavity leads to the active site, where the iron(II) centre is ligated by three amino acid sidechains: His-146, His-210 and Glu-260 (see Fig. 2D).¹¹ This His₂Glu/Asp motif is found in a number of other non-haem iron(II)-dependent oxygenases, including the α -ketoglutarate

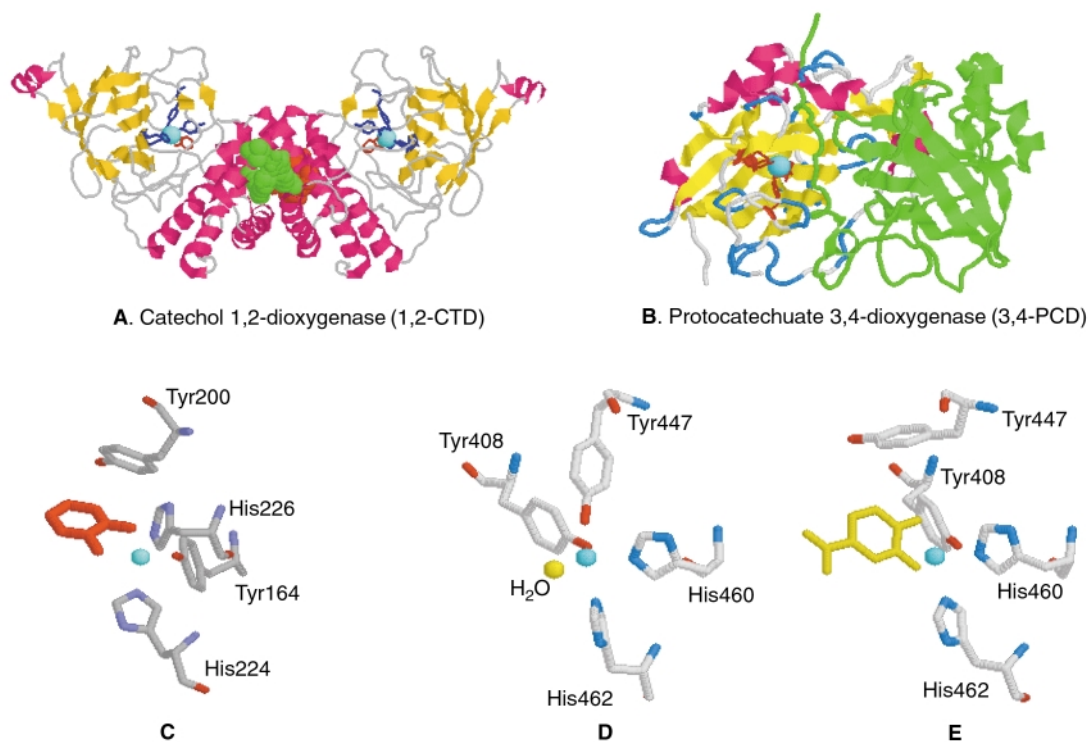


Fig. 1 X-Ray crystal structures of intradiol catechol dioxygenases. **A.** Catechol 1,2-dioxygenase (1,2-CTD) from *Acinetobacter* sp. ADP1,¹⁰ showing iron(III) cofactor, ligands, and bound substrate. Bound phospholipid in shaded green (PDB accession number 1DLT). **B.** Protocatechuate 3,4-dioxygenase (3,4-PCD) from *Pseudomonas putida*,⁷ showing α and β subunits (β subunit in green), iron(III) cofactor, ligands (PDB accession number 2PCD). **C.** Active site of 1,2-CTD,¹⁰ showing iron(III) cofactor, ligands, and bound catechol substrate (in red). **D.** Active site of 3,4-PCD,⁷ showing iron(III) cofactor and ligands. **E.** Active site of 3,4-PCD co-crystallised with analogue 2-hydroxyisonicotinic acid *N*-oxide (in yellow),¹⁷ illustrating the movement of Tyr-447 (PDB accession number 3PCL).

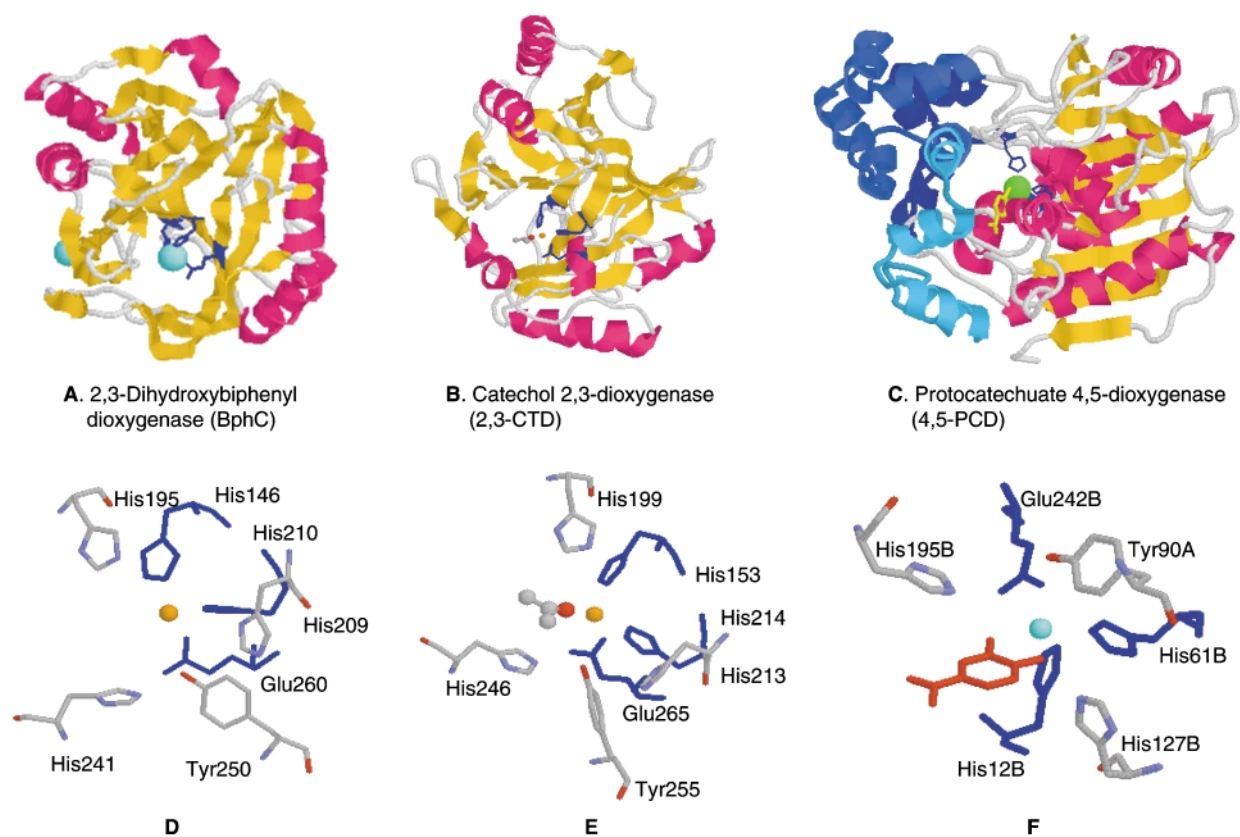


Fig. 2 X-Ray crystal structures of extradiol catechol dioxygenases. **A.** 2,3-Dihydroxybiphenyl 1,2-dioxygenase (BphC) from *Pseudomonas* LB400,¹¹ showing iron(II) cofactor and ligands (PDB accession number 1HAN). **B.** Catechol 2,3-dioxygenase (2,3-CTD) from *Pseudomonas putida* mt-2,¹⁴ showing the iron(II) cofactor, ligands, and a molecule of acetone bound to the iron centre (PDB accession number 1MPY). **C.** Protocatechuate 4,5-dioxygenase (LigAB) from *Sphingomonas paucimobilis* SYK-6,¹⁵ showing α and β subunits (α subunit in blue), iron(II) cofactor, ligands, and bound substrate (PDB accession number 1B4U). **D.** Active site of BphC,¹¹ showing iron(II) cofactor, ligands (in blue), and nearby active site residues. **E.** Active site of 2,3-CTD,¹⁴ showing iron(II) cofactor, ligands (in blue), bound acetone molecule, and nearby active site residues. **F.** Active site of LigAB,¹⁵ showing iron(II) cofactor, ligands (in blue), bound substrate protocatechuic acid (in red), and nearby active site residues.

dependent dioxygenases and isopenicillin N synthase.¹² The crystal structure of BphC from *Pseudomonas* KKS102 has also been solved with bound substrate, yielding a similar co-ordination geometry; however the crystallised form of the enzyme contains iron(III) rather than iron(II).¹³

The crystal structures of three other extradiol dioxygenases have now been solved. In 1998 Kita *et al.* reported the structure of catechol 2,3-dioxygenase from *Pseudomonas putida* mt-2, an α_4 tetramer.¹⁴ The subunit structure is very similar to that of BphC, and the iron(II) cofactor is bound by His-153, His-214 and Glu-265 (see Fig. 2B,2E).¹⁴ In 1999 Sugimoto *et al.* reported the structure of protocatechuate 4,5-dioxygenase from *Sphingomonas paucimobilis* SYK-6, which is composed of an $\alpha_2\beta_2$ tetramer.¹⁵ This enzyme has no sequence similarity to BphC, yet the disposition of iron(II) ligands is very similar: the metal centre is co-ordinated by His-12, His-61 and Glu-242 (see Fig. 2C,2F).¹⁵ In 2000 Titus *et al.* reported the structure of human homogentisate dioxygenase, a non-haem iron(II)-dependent dioxygenase involved in the mammalian degradation of L-phenylalanine and L-tyrosine.¹⁶ This enzyme bears no sequence similarity to the bacterial extradiol catechol dioxygenases, yet its active site features are very similar: the iron(II) cofactor is bound by His-335, Glu-341 and His-371.¹⁶

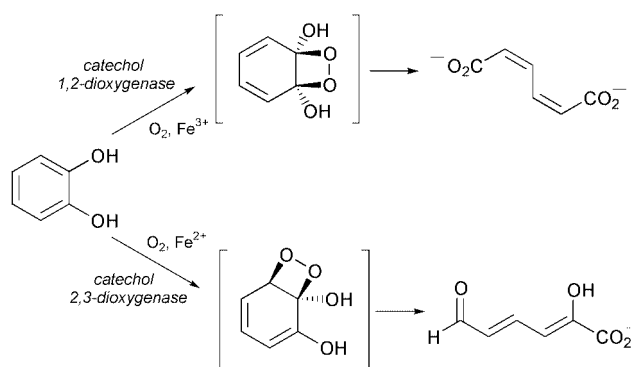
Thus, the solution of several X-ray structures has shown that each family of catechol dioxygenases has a specific set of amino acid ligands for the non-haem iron cofactor. The iron(III) cofactor of the intradiol dioxygenases is ligated by two tyrosine residues and two histidine residues, whereas the iron(II) cofactor of the extradiol dioxygenases is ligated by two histidine residues and one glutamic acid residue. Yet how does this small difference in co-ordination chemistry relate to the choice of reaction pathway? The active site structures do not reveal obvious differences which would explain why one yields the intradiol cleavage product and the other the extradiol cleavage product.

Furthermore, recent structures of co-crystals of protocatechuate 3,4-dioxygenase have demonstrated that the axial tyrosine ligand, Tyr-447, swings away from the iron(III) centre upon binding of substrate analogues, leaving only three amino acid ligands for the iron(III) centre (see Fig. 1E).¹⁷ The riddle of the intradiol *vs.* extradiol dioxygenases therefore becomes more intriguing: why Fe^{3+} and a His_2Tyr_2 motif (one of which appears to dissociate during the reaction) for intradiol cleavage, and why Fe^{2+} and a His_2Glu motif for extradiol cleavage?

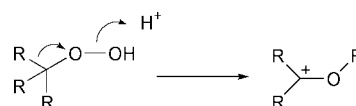
Evidence for 1,2 (Criegee) rearrangements in the catechol dioxygenases

The catalytic mechanism proposed by Hayaishi involved the formation of a cyclohexadienone hydroperoxide in both the intradiol and extradiol dioxygenases, followed by the formation of a four-membered dioxetane ring.⁴ Once formed, the strained dioxetane would readily undergo retro[2+2] cleavage to give the acyclic products, with complete incorporation of both atoms of oxygen from dioxygen (see Scheme 2). There was, however, some disquiet about this mechanism: the formation of dioxetanes was thought to be a highly endothermic process, and their breakdown should be accompanied by luminescence, which is not observed for the catechol dioxygenases.¹⁸ Indeed, the only well-characterised example of a dioxetane intermediate in an enzyme-catalysed reaction was the firefly luciferase reaction, in which decomposition of a dioxetane intermediate yields the luminescence characteristic of the firefly.¹⁹

An alternative mechanism involves a 1,2-rearrangement of the intermediate hydroperoxide. It is well precedented that alkyl hydroperoxides can undergo migration of a carbon substituent onto the neighbouring electron-deficient oxygen, with loss of the second oxygen atom *via* heterolytic O–O cleavage (see Scheme 3). In the case of an alkyl hydroperoxide this is known as a Criegee rearrangement.²⁰ This type of 1,2-rearrangement is



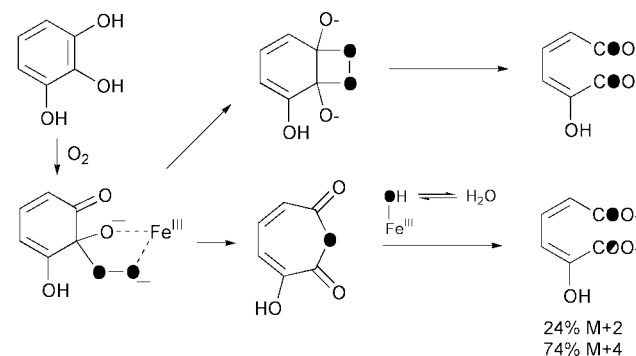
Scheme 2 Dioxetane intermediates proposed by Hayaishi for the catechol dioxygenases.



Scheme 3 1,2-Rearrangement of a hydroperoxide.

also commonly observed during the Baeyer–Villiger oxidation of ketones,²¹ where an intermediate hydroperoxide is formed upon attack of hydrogen peroxide or a peracid on a ketone.

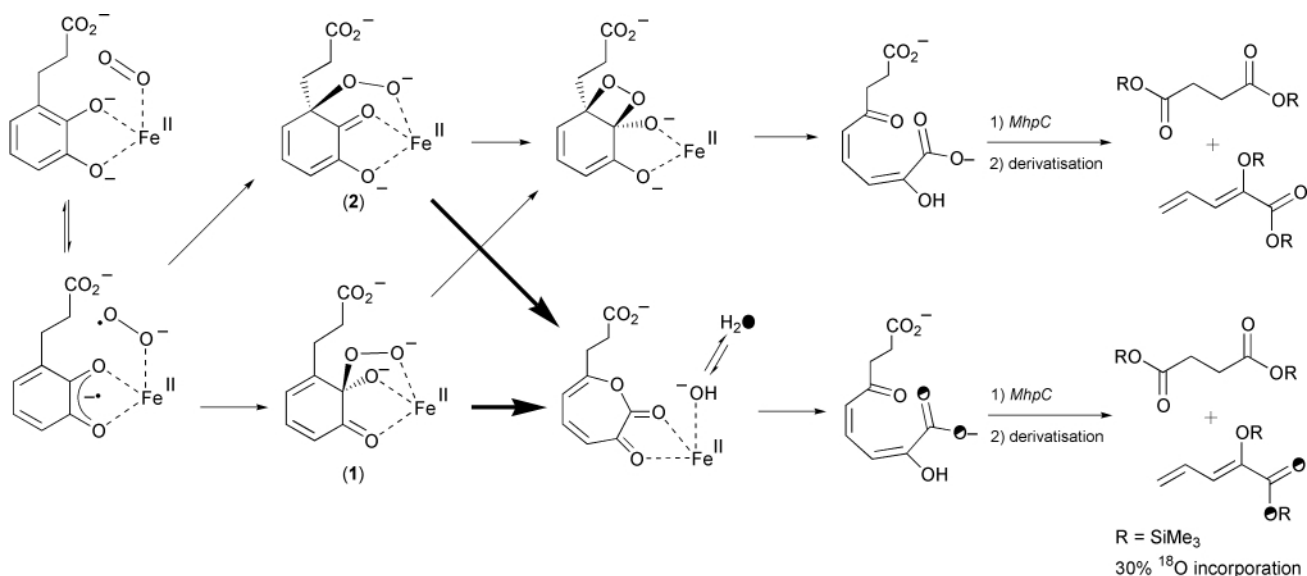
For intradiol cleavage, upon formation of a cyclohexadienyl hydroperoxide, migration of the adjacent acyl group (acyl migration) would yield muconic anhydride as an intermediate, which would undergo hydrolysis to give the product muconic acid. ¹⁸O₂ labelling studies on catechol 1,2-dioxygenase from *Pseudomonas arvilla* have revealed that the intradiol cleavage products contain 99% incorporation of a single atom of ¹⁸O, and 74% incorporation of a second atom of ¹⁸O, with 24% incorporation of only one atom of ¹⁸O (see Scheme 4).²² These



Scheme 4 ¹⁸O₂ labelling studies on the reaction of pyrogallol with catechol 1,2-dioxygenase from *Pseudomonas arvilla*.

data are not consistent with a dioxetane intermediate, but could be explained by a Criegee rearrangement to give an anhydride intermediate, followed by the partial exchange of the iron(III) ¹⁸O-hydroxide with solvent water.²² Interestingly, no single atom isotope incorporation is observed with the natural substrate catechol, implying a lack of exchange or a more efficient hydrolysis of the anhydride intermediate.²² Model reactions for intradiol cleavage (see below) have in some cases yielded muconic anhydrides as reaction products, again consistent with a 1,2-rearrangement.

In the case of extradiol cleavage, there are two possible cyclohexadienyl hydroperoxides which could undergo 1,2-rearrangements. The first possibility is that proximal hydroperoxide (**1**) is formed, as for intradiol cleavage, which undergoes migration of the adjacent alkene (alkenyl migration) to give an α -keto-lactone intermediate, which then undergoes hydrolysis by iron(II) hydroxide to give 2-hydroxymuconate semi-aldehyde. The second possibility is that a distal hydro-



Scheme 5 Mechanistic schemes for MhpB-catalysed reaction showing ¹⁸O labelling pattern.

peroxide (**2**) is formed, which undergoes 1,2-rearrangement *via* acyl migration to give the same α -keto-lactone intermediate (see Scheme 5). ¹⁸O₂ labelling studies carried out on *E. coli* 2,3-dihydroxyphenylpropionate 1,2-dioxygenase (MhpB) revealed that although both the acid and ketone carbonyls could be labelled with ¹⁸O from ¹⁸O₂, upon reaction in H₂¹⁸O the carboxylate position was labelled to the extent of 30%, consistent with the formation of an α -keto lactone intermediate, and exchange of iron(II) hydroxide with solvent ¹⁸O-labelled water (see Scheme 5).²³ The enzyme was also found to catalyse the hydrolysis of a saturated seven-membered lactone analogue (**3**; see Scheme 6).²³ These studies implicate a lactone intermediate arising from Criegee rearrangement in the extradiol cleavage reaction mechanism.

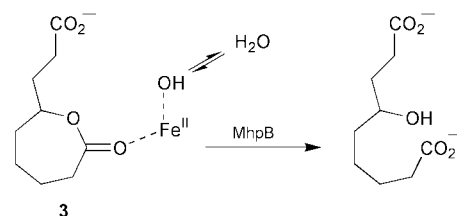
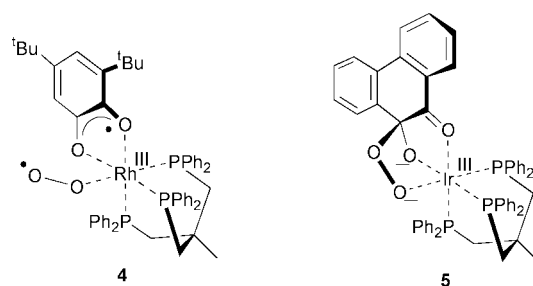
Thus, evidence from ¹⁸O labelling experiments and model studies has revealed that both intradiol and extradiol cleavage reactions involve 1,2-rearrangements taking place on cyclohexadienyl hydroperoxide reaction intermediates, in close proximity to the non-haem iron cofactors.

Formation of cyclohexadienyl hydroperoxides *via* single electron transfers

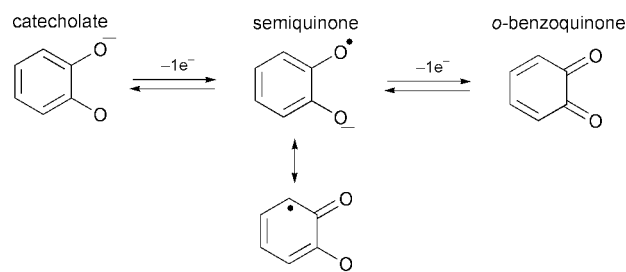
The formation of cyclohexadienyl hydroperoxides is implicated in both intradiol and extradiol cleavage reactions from the studies discussed above. How are they formed? What are the differences between the Fe³⁺-based intradiol reaction and the Fe²⁺-based extradiol reaction?

There are several clues from known chemistry that single electron transfers may be involved in each case. First of all, it is well established that the triplet ground state of dioxygen is forbidden to react with paired-electron reagents, however it can react with radical species, and it can accept one electron from certain transition metal ions to form the much more reactive superoxide species.²⁴ Indeed, there are many examples of divalent transition metals (*e.g.* Fe^{II}, Co^{II}, Ir^{II}) which can form stable metal(III)-superoxide complexes upon reaction with dioxygen.²⁴ The next clue is that catechol readily undergoes single electron oxidation, *via* a stable semiquinone intermediate, to an *ortho*-quinone species (see Scheme 7). Thus, a redox-active metal such as iron could mediate one-electron transfers between catechol and dioxygen.

There are specific examples from transition metal chemistry which suggest that this may be the case. The X-ray crystal structure of a rhodium(III)-triphos-catecholate complex (**4**) with dioxygen synthesised by Bianchini *et al.* shows that dioxygen is bound as superoxide, and that catechol is bound as



Scheme 6 Lactone hydrolysis catalysed by MhpB.



Scheme 7 Single electron oxidation of catechol.

its semiquinone.²⁵ This metal-semiquinone-superoxide complex could be formed by one-electron transfer from Rh^{III} to dioxygen, followed by one-electron transfer from catechol to Rh^{II}. The X-ray structure of the corresponding iridium(III) complex (**5**) shows a C–O bond formed between the catechol ring and dioxygen,²⁶ indicating that C–O bond formation between metal-bound semiquinone and metal-bound superoxide is feasible, to give a cyclohexadienyl hydroperoxide. A similar cyclohexadienyl hydroperoxide has been reported for a

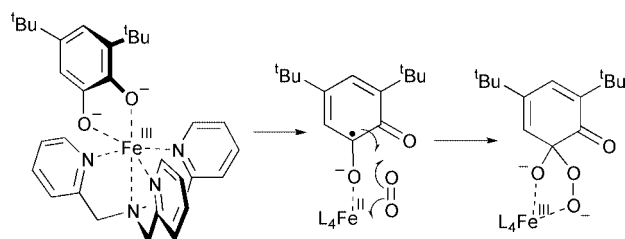
Rh^{III} complex, formed by reaction of Rh^I(PPh₃)₃Cl with 9,10-phenanthrenequinone.²⁷ One final clue for the involvement of superoxide is the existence of a model reaction for catechol cleavage involving treatment of catechol in DMSO with solid potassium superoxide, which gives a 5–10% yield of 2-hydroxy-muconic semialdehyde, the extradiol cleavage product.²⁸

EPR spectroscopic studies have shown that the iron(III) cofactor of the intradiol dioxygenase family ligates to the catechol hydroxy groups, by displacement of a bound water molecule; however no transient iron(II) intermediates are detectable during turnover.^{29,30} EPR spectroscopic studies of the NO complex of the extradiol dioxygenase protocatechuate 4,5-dioxygenase have shown that the iron(II) cofactor binds both catecholic hydroxy groups, and binds NO; however no iron(III) intermediates could be detected during turnover.³¹ Thus, EPR spectroscopy has provided no experimental evidence for the involvement of one-electron transfers in the catechol dioxygenase reactions. However, if the one-electron transfers were very fast, then no build-up of intermediates would be observable.

The existence of carbon-centred radicals in enzyme-catalysed reactions has been probed in several cases using 'radical trap' substrates containing a cyclopropyl group adjacent to the radical-bearing carbon atom.³² Formation of the radical intermediate would then lead to an extremely rapid opening of the cyclopropane ring, yielding a new reaction product or leading to enzyme inactivation. A cyclopropyl-containing substrate analogue (**6**) was synthesised as a substrate for 2,3-dihydroxyphenylpropanate 1,2-dioxygenase (MhpB) from *E. coli*.³³ Both *cis*- and *trans*-substituted cyclopropyl analogues were found to be efficiently processed by the enzyme. However, when the products were analysed by further enzymatic degradation, it was found that isomerisation of the cyclopropyl ring substituents had occurred: processing of the *trans*-substituted substrate gave 94% *trans*-product and 6% *cis*-product; while processing of the *cis*-substituted substrate gave only 10% of the *cis*-product, and 90% of the *trans*-product (see Scheme 8). Having established that epimerisation *via* solvent exchange was not occurring, the only reasonable explanation of these results is that a radical-mediated reversible opening of the cyclopropyl ring is taking place.³³ Since the equilibrium position of ring-closed *vs.* ring-opened product is governed by the stability of

ring-closed *vs.* ring-opened products, the reversible ring opening can be explained by the high stability of the initial semiquinone radical. These data provide some experimental evidence for a transient iron(II)–semiquinone–superoxide intermediate in the extradiol catechol dioxygenase reaction mechanism.

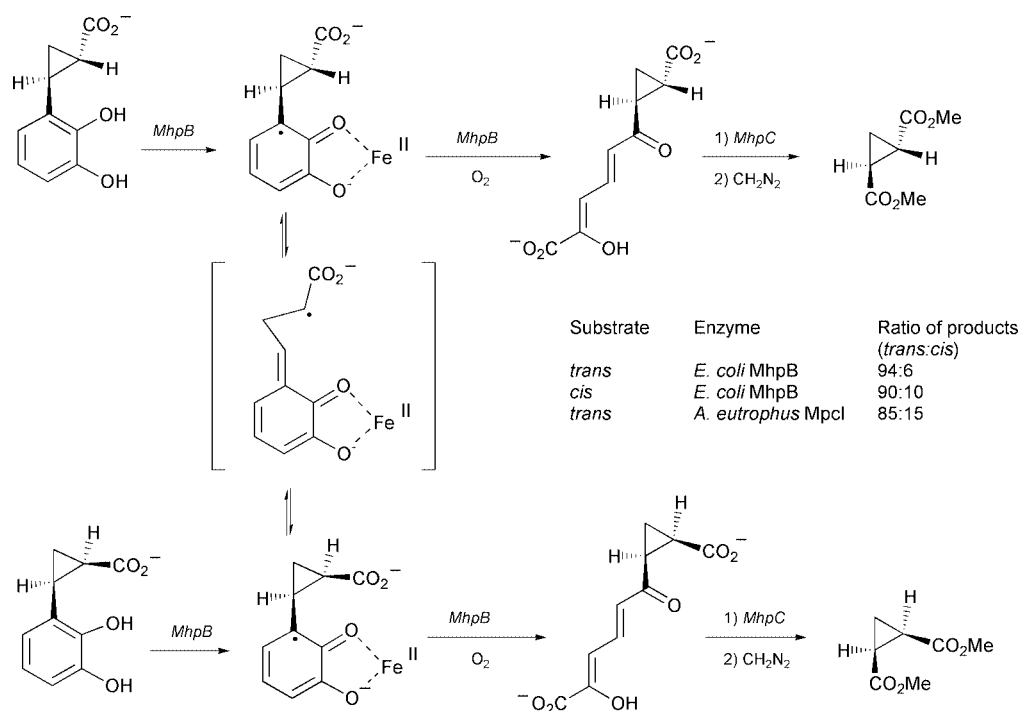
Evidence from model studies of intradiol cleavage also suggests the involvement of one-electron transfers. Analysis of a Fe^{III}tris(2-pyridylmethyl)amine complex (**7**), which showed high activity for intradiol catechol cleavage, by X-ray crystallography and ¹H NMR spectroscopy revealed a very strong iron–catecholate interaction, and increased semiquinone character in the bound substrate.^{34,35} It was therefore proposed that formation of a transient Fe^{II}–semiquinone intermediate preceded reaction with dioxygen (see Scheme 9).³⁵ Since no



Scheme 9 Semiquinone activation proposed for intradiol cleavage.

binding of O₂ or NO to the iron(III) centre of the intradiol dioxygenases has been observed by EPR spectroscopy,^{29,30} it is proposed that the iron(II)-bound semiquinone reacts directly with dioxygen, without prior binding of dioxygen to the iron centre.³⁵

Thus, both intradiol and extradiol dioxygenases utilise single electron transfers to form a cyclohexadienyl hydroperoxide intermediate, although the order of steps is different in the two enzymes. In the extradiol dioxygenase active site single electron transfer from iron(II) to dioxygen is followed by single electron transfer from catechol to iron(III), to give a transient iron(II)–semiquinone–superoxide intermediate, which then undergoes C–O bond formation. In the intradiol dioxygenase active site single electron transfer from catechol to iron(III) gives an iron(II)-semiquinone intermediate which reacts directly with dioxygen to form the C–O bond. Both families make use of the



Scheme 8 *Cis*–*trans* isomerisation of a cyclopropyl radical trap (**6**) catalysed by extradiol dioxygenase MhpB.

single electron redox chemistry of iron and catechol, but *via* a different sequence.

Evidence for a proximal hydroperoxide in the extradiol catechol dioxygenases

Returning to the cyclohexadienyl hydroperoxide intermediate formed after the single electron redox chemistry described above, there is one important issue to be resolved. The extradiol cleavage mechanism could proceed *via* either of two possible cyclohexadienyl hydroperoxides (Scheme 5). As discussed in Section 3, either a proximal hydroperoxide could undergo alkenyl migration to give an α -keto-lactone, or a distal hydroperoxide could undergo acyl migration to give the same α -keto-lactone. Which is it?

Several pieces of circumstantial evidence favour the intermediacy of a proximal hydroperoxide, rather than a distal hydroperoxide. Inspection of models reveals that the geometry required to form the distal hydroperoxide is rather strained, and inspection of the X-ray structures of BphC also indicates that reaction at the proximal position of the substrate is more readily achievable than reaction at the distal position.^{11,13} The iridium(III) model complex (**5**) containing a cyclohexadienyl hydroperoxide also exhibits a proximal hydroperoxide.²⁶

More definitive evidence has been obtained for the extradiol dioxygenase 2,3-dihydroxyphenylpropionate 1,2-dioxygenase (MhpB) from *E. coli*. It was known from structure-activity relationships that MhpB would process substrates containing a diverse range of functional groups at the 3-position (*e.g.* alkyl,

$-\text{CH}=\text{CHCO}_2\text{H}$, $-\text{OCH}_2\text{CO}_2\text{H}$) with comparable efficiency, which is hard to reconcile with the formation of a distal hydroperoxide at the 3-position.³³ A series of analogues of the proximal and distal hydroperoxides were synthesised, in which the $-\text{OOH}$ functional group was replaced by $-\text{CH}_2\text{OH}$, and the cyclohexadienyl ring simplified to a cyclohexanone ring.³⁶ These 'carba' analogues are shown in Fig. 3. It was found that the carba analogue **7** of the distal hydroperoxide showed no inhibition of MhpB at 10 mM concentration. However, analogues **9** and **10** of the proximal hydroperoxide did show modest competitive inhibition of MhpB, with K_i values of 4.9 mM and 0.7 mM respectively. In contrast, the methyl-substituted analogue **8** showed no enzyme inhibition. Analysis by ^1H NMR spectroscopy revealed that in **9** and **10** the hydroxymethyl substituent is positioned in an axial orientation with respect to the cyclohexanone ring, whereas in **8** the hydroxymethyl group was equatorial (see Fig. 3).³⁶ These data provided some experimental evidence in support of a proximal hydroperoxide, and furthermore indicated that the conformation adopted by the hydroperoxide was of importance, an axial hydroperoxide being required at the extradiol dioxygenase active site.

This result has an important consequence for the reaction mechanisms of both families of enzyme, namely that both reactions converge on the same proximal cyclohexadienyl hydroperoxide intermediate (see Fig. 4). In the case of the intradiol dioxygenases, this intermediate undergoes acyl migration to give a muconic anhydride, whereas in the extradiol dioxygenases the proximal hydroperoxide undergoes alkenyl migration to give an α -keto-lactone. Therefore, in spite of the differences in the early steps of the reaction mechanism, the inescapable conclusion is that the choice of intradiol *vs.* extradiol reaction pathways is controlled by the choice of acyl *vs.* alkenyl migration of a reactive proximal hydroperoxide intermediate. How might this choice of 1,2-rearrangements be controlled?

Acyl *vs.* alkenyl migration in hydroperoxide rearrangements

In order to address the question of acyl *vs.* alkenyl migration, we must first look at examples of hydroperoxide rearrangements in organic chemistry. This section will describe instructive examples from Criegee rearrangements and Baeyer-Villiger oxidations.

The first example which provides a good model for the desired proximal hydroperoxide occurs in the Baeyer-Villiger oxidation of 1,2-diketones, in which anhydride products are formed in a range of examples.²¹ Thus, upon attack of peroxide or a peracid upon one ketone centre, an intermediate α -keto-hydroperoxide is formed, which undergoes acyl migration (see Scheme 10). This example provides clear precedent for the acyl migration step of intradiol cleavage, to give an anhydride

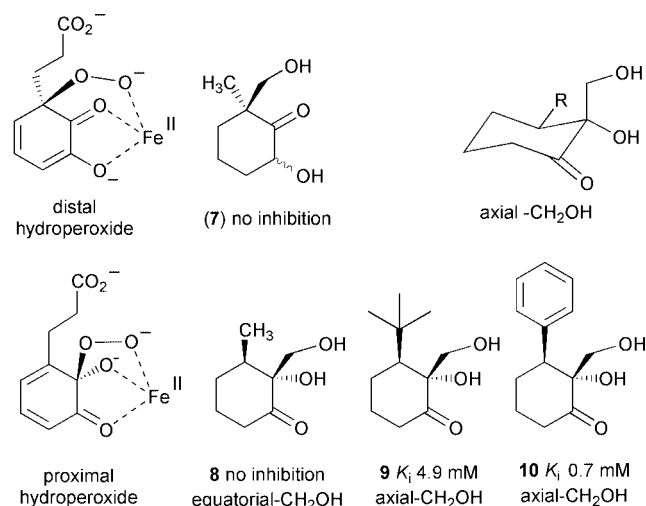


Fig. 3 Carba analogues of proximal and distal hydroperoxide reaction intermediates, tested as inhibitors for 2,3-dihydroxyphenylpropionate 1,2-dioxygenase (MhpB) from *Escherichia coli*.³⁶

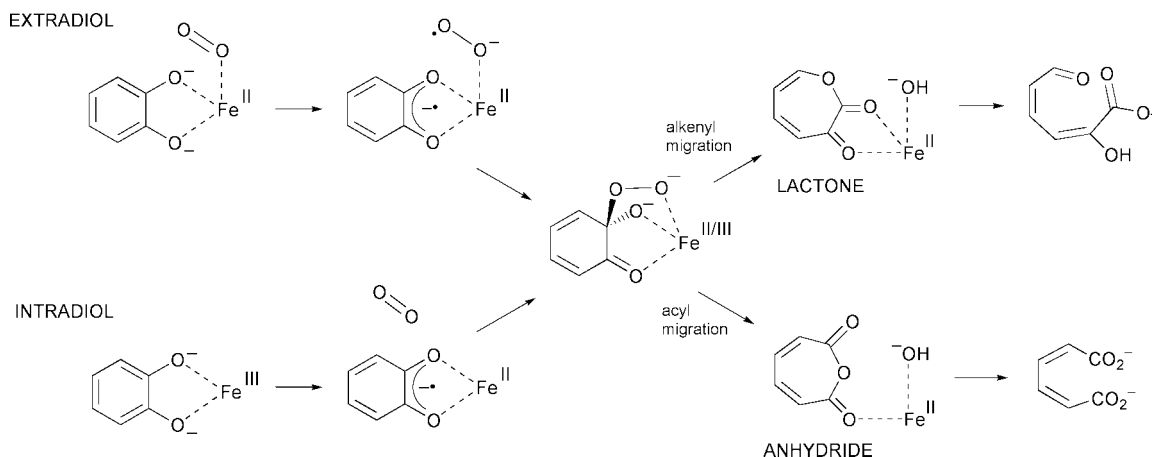
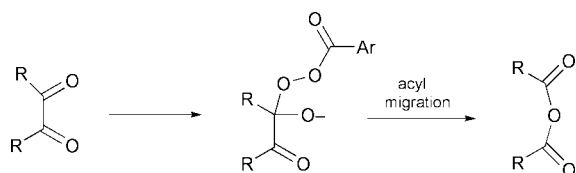
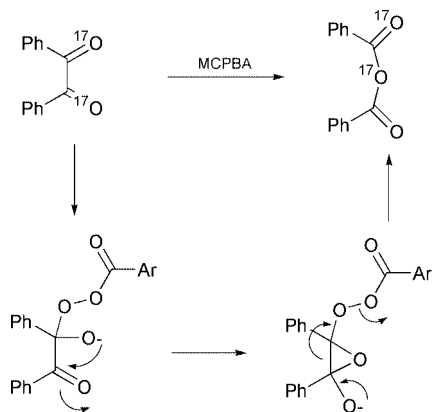


Fig. 4 Proposed mechanistic convergence of the catalytic mechanisms of the extradiol and intradiol catechol dioxygenases onto a common proximal hydroperoxide intermediate, and their divergence *via* alkenyl or acyl migration to give extradiol or intradiol reaction products.



Scheme 10 Baeyer–Villiger oxidation of 1,2-diketones.

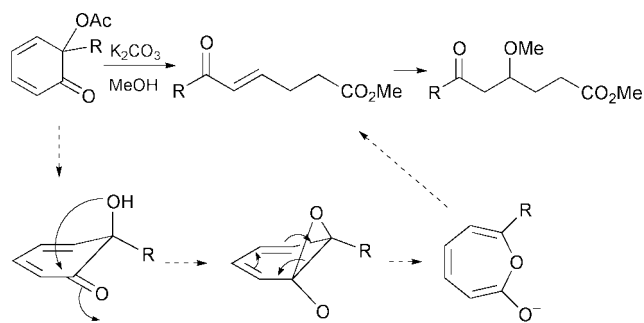
product. However, the mechanism of acyl migration may not be as straightforward as it seems. Baeyer–Villiger oxidation of ^{17}O -labelled benzil gave anhydride product containing ^{17}O in the bridging position, not consistent with a direct migration of an acyl group (see Scheme 11).³⁷ A mechanism was proposed



Scheme 11 Epoxide mechanism proposed for Bayer–Villiger oxidation of benzil.

involving attack of the alkoxide ion upon the adjacent ketone, to form a 1,2-epoxide, followed by C–C fragmentation to give the anhydride product (see Scheme 11).³⁷ It is known that the presence of electron-withdrawing groups reduces migratory aptitude in Baeyer–Villiger oxidations,³⁸ therefore the facile migration of an electron-deficient acyl group in this case could be rationalised by this alternative mechanism.

One recent observation suggests that such a mechanism might operate in the acyl migration of cyclohexadienyl hydroperoxides. Treatment of 6-alkyl-6-acetoxycyclohexa-2,4-dienones with carbonate buffer in water–methanol leads to a rapid C–C cleavage reaction, resulting in the production of acyclic esters (see Scheme 12). Studies of the mechanism of this

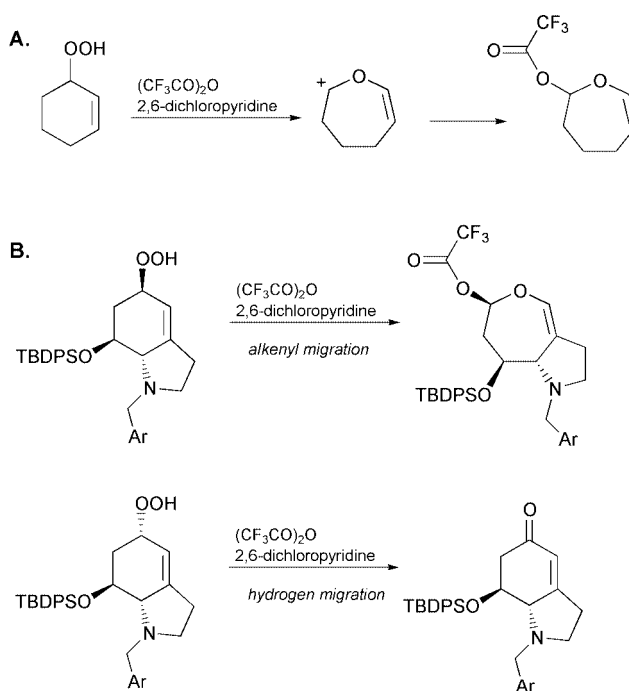


Scheme 12 Solvolytic C–C cleavage of 6-alkyl-6-acetoxycyclohexa-dienones (R = CH₃, Ph).

C–C cleavage reaction indicate that hydrolysis of the acetyl group is essential for ring cleavage, hence that a mechanism involving attack of the tertiary alcohol on the adjacent ketone, followed by a benzene oxide–oxepin interconversion, may mediate ring cleavage in this system (see Scheme 12). This mechanism provides an alternative pathway for acyl migration in the intradiol dioxygenase reaction.³⁹

Recent work by Goodman and Kishi provides clear examples of alkenyl migration: treatment of a cyclohexenyl hydroperoxide with trifluoroacetic anhydride yields products arising from alkenyl migration in preference to alkyl migration (see

Scheme 13A).⁴⁰ In cases where the hydroperoxide group is positioned on a bicyclic carbon skeleton, as shown in Scheme 13B, the choice of migrating group is determined by stereoelec-



Scheme 13 Alkenyl migration of a cyclohexyl hydroperoxides.

tronic factors: the group which preferentially migrates is the one which is positioned anti-periplanar to the O–O bond which is being broken,⁴⁰ as one might expect from stereoelectronic arguments.⁴¹

This idea provides an attractive rationalisation of the results obtained using the carba-analogues of proximal hydroperoxide intermediates in the MhpB-catalysed reaction.³⁶ If the hydroperoxide functional group is positioned axially with respect to the cyclohexadienone ring, and is ligated to the iron(II) centre, then the O–O bond will be aligned in an antiperiplanar geometry with the C–C bond to the neighbouring alkenyl group which migrates in the extradiol reaction (see Fig. 5A). Thus, one factor

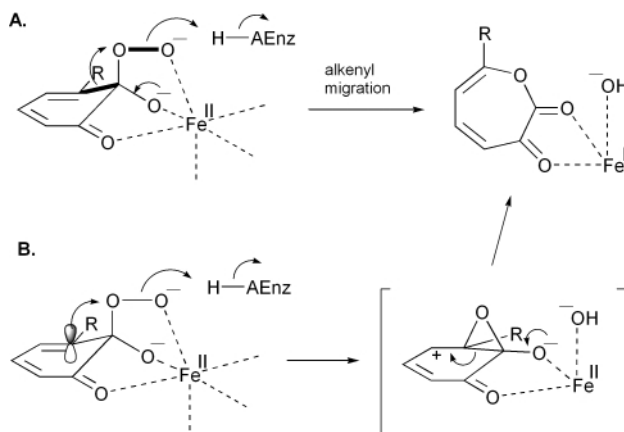
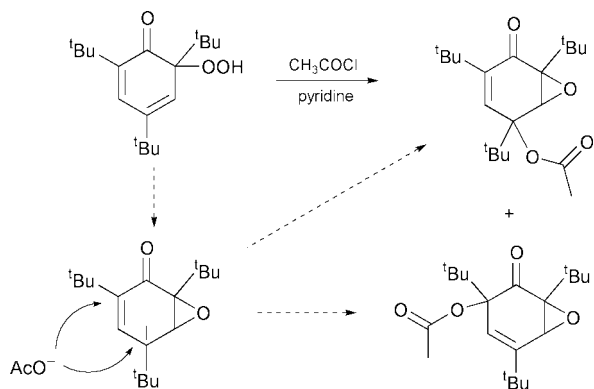


Fig. 5 Two possible mechanisms for alkenyl migration in the extradiol dioxygenase reaction pathway. **A.** σ bond migration of an axial hydroperoxide. **B.** π participation mechanism.

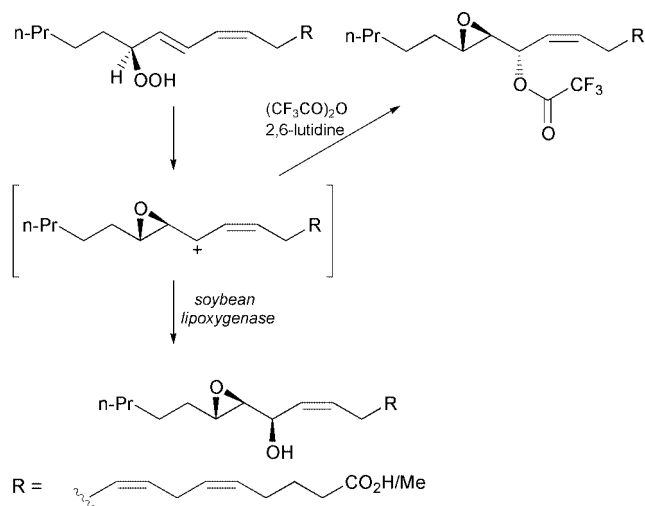
which could control the acyl vs. alkenyl migration of a common hydroperoxide intermediate is the conformation of the bound intermediate and hence precise positioning of the O–O bond.

Further reactions of alkenyl hydroperoxides provide an alternative mechanism for alkenyl migration. Nishinaga *et al.* have reported that treatment of a tributyl-substituted cyclohexadienone hydroperoxide with acetyl chloride–pyridine leads to the formation of two epoxides (see Scheme 14).⁴² These



Scheme 14 Epoxide formation in cyclohexadienyl hydroperoxide rearrangement.

epoxides could be formed by nucleophilic participation of the neighbouring alkene to form an epoxide intermediate containing an allylic carbocation, which could be quenched by acetate. Note that in this case the *tert*-butyl substituent will ensure that the hydroperoxide is held axially with respect to the ring, which would bring the hydroperoxide in close proximity to the π system of the neighbouring diene. Further examples of the reaction of polyunsaturated fatty acid hydroperoxides to form epoxides have also been reported by Corey *et al.* (see Scheme 15).^{43,44} Again an adjacent diene is present, so that the intermediate carbocation arising from nucleophilic participation would be a stabilised allylic carbocation.



Scheme 15 Epoxide formation in polyunsaturated fatty acid hydroperoxide rearrangement.

This π participation mechanism could be applied to the alkenyl migration step of the extradiol reaction pathway.³⁶ If the hydroperoxide functional group is held axially with respect to the cyclohexadienone ring, then the π system of the diene would overlap with the σ^* orbital of the O–O bond, leading to the formation of a transient epoxide species bearing an adjacent allylic carbocation, which would rapidly undergo C–C fragmentation to give the α -keto-lactone (see Fig. 5B). Thus, there are two subtly different mechanisms for alkenyl migration of an axial proximal hydroperoxide: either σ bond migration of an antiperiplanar alkenyl group, or π participation of the adjacent diene.

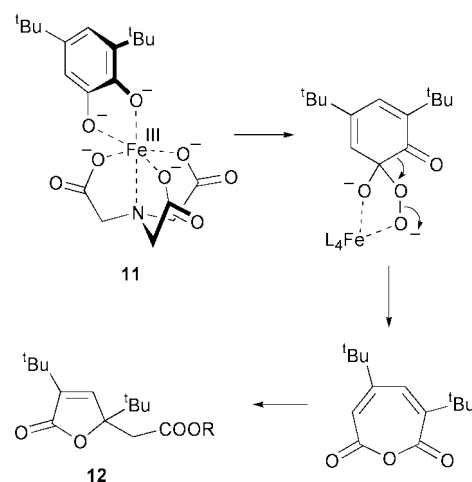
In conclusion, there are literature examples of both acyl migration and alkenyl migration in hydroperoxide 1,2-rearrangements in organic chemistry. The control of migratory group *via* stereoelectronic factors would provide an attractive means by which an enzyme active site might dictate intradiol *vs.* extradiol cleavage. However, the examples in this Section lack one crucial feature of the enzyme-catalysed reactions: the proximity of the non-haem iron centre, whose effects upon intradiol *vs.* extradiol cleavage will be discussed next.

Transition metal-based model reactions for oxidative catechol cleavage

Since the discovery of the catechol dioxygenases, many attempts have been made to mimic these reactions non-enzymatically. The intriguing iron cofactor specificity of the catechol dioxygenase suggested that the iron cofactor played a major role in the active site chemistry, hence most attempts have involved metal ion complexes of catechol substrates. Does the character of the iron centre control the choice of cleavage pathways?

Model systems for intradiol cleavage

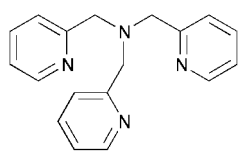
The first model system for intradiol cleavage was an Fe^{III}-nitritotriacetate complex **11**, which was reported to convert 3,5-di-*tert*-butylcatechol catalytically over a period of 4 days in the presence of oxygen to give the furanone derivative **12** in 80% yield.^{45,46} An X-ray crystal structure of this complex showed the catechol substrate bound in bidentate fashion, with the geometry around the central Fe^{III} close to octahedral.⁴⁶ Labelling studies with ¹⁸O₂ on this system revealed the incorporation of one atom of ¹⁸O₂ into furanone **12**, consistent with the existence of an anhydride intermediate as shown in Scheme 16.⁴⁶



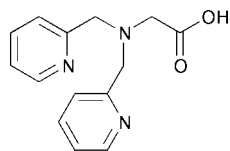
Scheme 16 Intradiol cleavage catalysed by Fe^{III}(NTA) complex **11**.

Subsequent studies using a range of iron(III) complexes showed a correlation between the reactivity of the Fe^{III}-ligand system and the Lewis acidity of the metal centre, which could be quantitatively assessed by measuring the redox potential for the catechol-to-semiquinone oxidation.⁴⁷ Of the complexes studied, the Fe^{III}-nitritotriacetate complex **11** showed the highest reactivity, and the highest redox potential of +59 mV (and hence the highest affinity of the catechol ligand for the Fe^{III} centre).⁴⁷

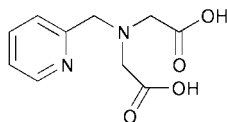
Further studies by Que and co-workers led to the discovery of more reactive Fe^{III} complexes,^{34,35} the most active of which was Fe^{III}-tris(2-pyridylmethyl)amine **13**. This complex was found to react with dioxygen within minutes to form furanone **12** in 98% yield, at a rate of 15 M⁻¹ s⁻¹, approximately 1000-fold faster than complex **11**. Analysis of complex **13** by X-ray crystallography and ¹H-NMR spectroscopy revealed a very strong iron-catechol interaction, and increased semiquinone character in the bound substrate. It was therefore proposed that formation of a transient Fe^{II}-semiquinone intermediate preceded reaction with dioxygen, as shown previously in Scheme 9. Each of these tetradentate ligands **13–16**, when complexed to Fe^{III}, showed activity for intradiol cleavage, revealing that two easily accessible *cis* coordination sites are needed for coordination of the catecholate ligand and its subsequent reaction with dioxygen. The order of reactivity of the coordinated 3,5-di-*tert*-butylcatecholate ligand (dbc)²⁻ was in the order [Fe(**13**)(dbc)]⁺ > [Fe(**14**)(dbc)]⁺ > [Fe(**15**)(dbc)]⁺ > [Fe(**16**)(dbc)]⁺, and is correlated to the Lewis acidity of the iron(III) centre.^{34,35,45}



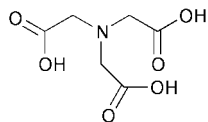
(13; TPA)



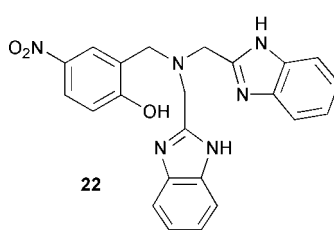
(14; BPG)



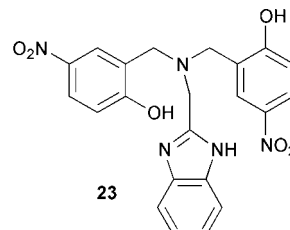
(15; PDA)



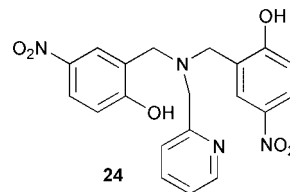
(16; NTA)



22

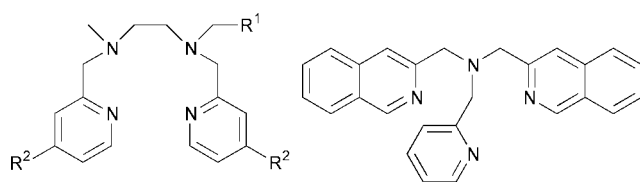


23

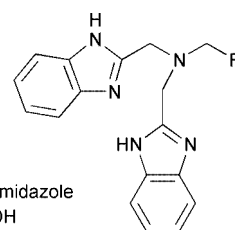


24

Girerd and co-workers have investigated the structures and reactivity of Fe^{III} complexes of **17–20** with 3,5-di-*tert*-butylcatechol, which all formed [Fe(L)(dbsq)] complexes with

17 R¹ = H, R² = H18 R¹ = H, R² = Cl19 R¹ = 2-pyridyl, R² = H

20

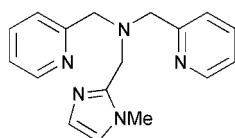


25 R = benzimidazole

26 R = CH₂OH

significant semiquinone character.⁴⁸ Reactivity for intradiol cleavage was found to correlate inversely with the λ_{\max} value, the order of reactivity being **13** (874 nm) > **17** (935 nm) > **18** (941 nm) > **19** (957 nm).⁴⁸

In most studies, 3,5-di-*tert*-butylcatechol has been used as a model substrate in functional investigations, however Krebs and co-workers have reported studies of iron(III) complexes of bis[(2-pyridyl)methyl][(1-methylimidazole-2-yl)methyl]amine **21** with a series of catechols.⁴⁹ The position of the ligand-metal



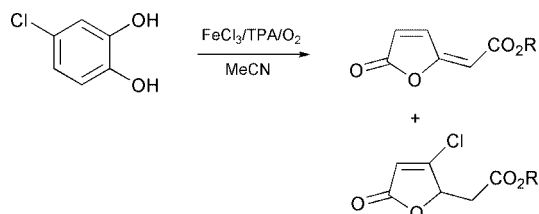
21

charge-transfer (LMCT) bands were observed to shift to lower energies by varying the substituents on the catecholate from electron-withdrawing to electron-donating. The reaction with dioxygen exhibits pseudo-first-order kinetics, and the order of activity correlates with the energy of the lower energy LMCT band of the complexes: electron-donating substituents on the catechol result in a higher dioxygenase activity.⁴⁹

Palaniandavar *et al.* have studied a series of iron(III) complexes of tetradentate tripodal ligands **22–24**, and found that not only the phenolate-to-iron(III) charge transfer band but also the L²⁻/dbc²⁻ to Fe^{III} charge transfer band is remarkably sensitive to the primary ligand environment.⁵⁰ The simultaneous appearance of the dbc²⁻ to Fe^{III} charge transfer band, the dbsq/dbc redox wave, and the lowering of the Fe^{III}/Fe^{II} redox potential on adding dbcH₂, even in the absence of added base, demonstrate the spontaneous deprotonation of the catechol substrate on binding to iron(III). Thus it is suggested that one function of the iron(III) center is to promote the loss of both protons of the substrate.⁵⁰

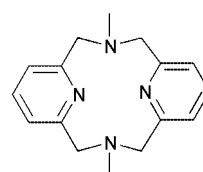
Attempts to mimic the ligating abilities of histidine in the active site of the enzyme have been reported, by introducing benzimidazole moieties into a tripodal ligand.⁵¹ Ligands **25,26** showed intradiol cleaving activity when complexed to Fe^{III}, the

reaction rate depending on the steric and electronic properties of the coordinating ligand moieties.⁵¹ Funabiki *et al.* have reported the first example of the oxidative cleavage of 3- and 4-chlorocatechols with dioxygen by an Fe^{III}(tpa) complex.⁵² 4-Chlorocatechol was oxygenated at 25 °C in acetonitrile under an oxygen atmosphere by the iron complex prepared *in situ* by mixing FeCl₃ and tris(2-pyridylmethyl)amine (tpa), giving rise to intradiol cleavage products as shown in Scheme 17.⁵²



Scheme 17

Finally, Kruger *et al.* have reported a highly reactive and catalytically active model system by using *N,N'*-dimethyl-2,11-diaza[3,3](2,6)pyridinophane (**27**, L-N₄Me₂) as a macro-



27

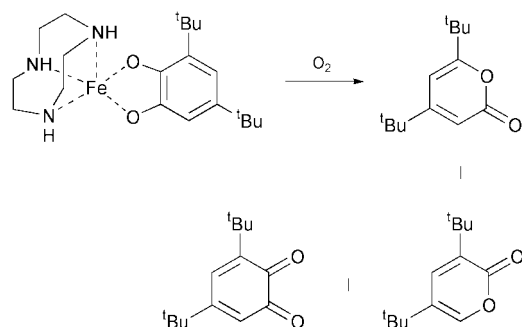
cyclic ligand.⁵³ For catalytic reaction, two equivalents of a base are needed per iron(III). With 1% of the iron(III) catalyst, a yield of 54% of muconic anhydride was obtained after a reaction time of 30 h.⁵³

In summary, intradiol cleavage activity is observed with a number of tetradentate nitrogen ligands, complexed to Fe^{III}. High activity is correlated with Lewis acidity of the Fe^{III} centre, and semiquinone character of the bound catechol substrate. The tetradentate co-ordination geometry of these systems parallels the tetradentate Fe^{III} co-ordination state in the intradiol dioxygenase active sites (see Fig. 1).

Model systems for extradiol cleavage

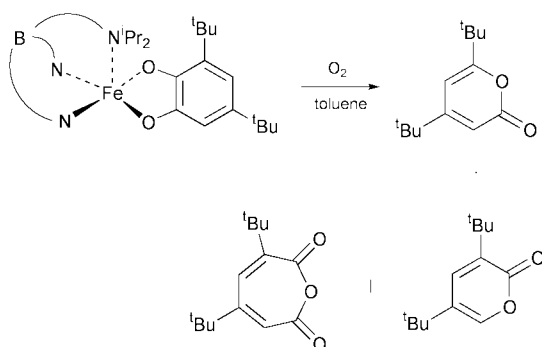
Although most of model reactions for catechol oxidative cleavage perform intradiol cleavage, there are a few examples of oxidative cleavage by synthetic iron complexes to give 2-pyrone products which are believed to be of extradiol origin, although they are lacking one carbon atom. Funabiki *et al.* found that $\text{FeCl}_2/\text{FeCl}_3$ complexes with bipyridine/pyridine prepared *in situ* cleave 3,5-di-*tert*-butylcatechol to give a mixture of 2-pyrones, which incorporate ^{18}O label from $^{18}\text{O}_2$.⁵⁴ The 2-pyrones are proposed to derive from decarbonylation of the α -keto-lactone extradiol cleavage intermediate.⁵⁴

Dei *et al.* found that the complex $[\text{Fe}^{\text{II}}(\text{TACN})(\text{dbc})]\text{Cl}$ (**28**) yielded 2-pyrones upon exposure to O_2 in 35% yield (see Scheme 18).⁵⁵ Que *et al.* used the same complex to give an



Scheme 18

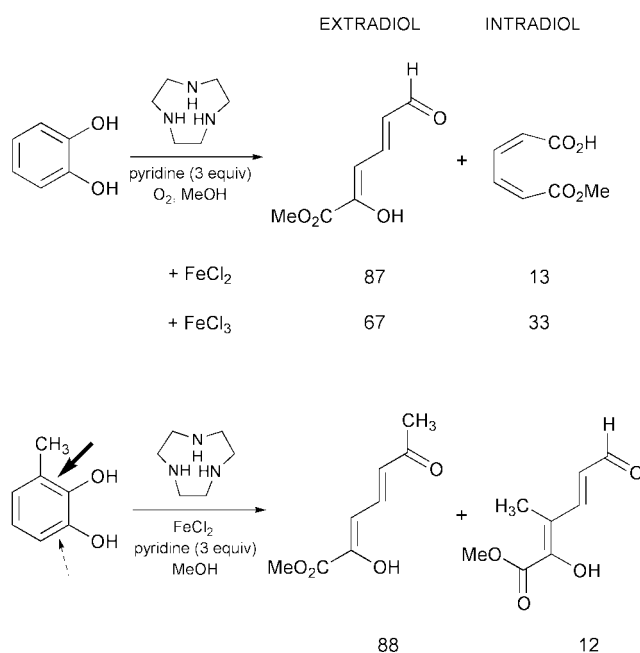
almost quantitative yield of 2-pyrones using a modified procedure with additional base/ligand in favor of extradiol cleavage.⁵⁶ Moro-oka *et al.* found that oxygenation of the square pyramidal complex $[\text{Fe}^{\text{III}}(\text{hydrotris}(3,5\text{-diisopropyl-1-pyrazoyl})\text{borate})(\text{dbc})]\text{Cl}$ (**29**) results in the formation of 2-pyrones and an intradiol-derived anhydride (see Scheme 19).⁵⁷ They report that a related complex which adopts a



Scheme 19

trigonal bipyramidal geometry gives no 2-pyrone products, therefore a vacant co-ordination site appears to be required for oxygen activation.⁵⁷

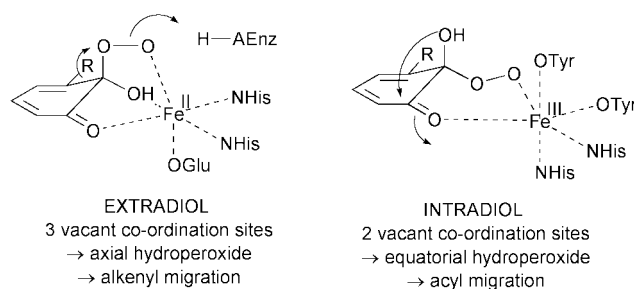
We have reported that the oxygenation of catechol by O_2 in the presence of FeCl_2 or FeCl_3 , 1,4,9-triazacyclononane (TACN), and pyridine in methanol gives the authentic extradiol product 2-hydroxymuconic semi-aldehyde methyl ester in 50% yield.⁵⁸ In this model system FeCl_2 -TACN shows higher selectivity for extradiol:intradiol cleavage (7:1) compared with FeCl_3 -TACN (2:1), as shown in Scheme 20. Extradiol cleavage is only observed with the facial N_3 -tridentate ligand TACN, and not with N,O-macrocycles, nor with N-substituted TACN macrocycles. We have found that this model reaction is highly regioselective for proximal 2,3-extradiol cleavage over distal 1,6-extradiol cleavage when using 3-methylcatechol (35:1), or 4-methylcatechol (>99), or 3-(2,3-dihydroxyphenyl)propionic acid (>99:1) as substrates.⁵⁹ The reaction proceeds in the absence of pyridine using monosodium



Scheme 20 FeCl_2 -TACN model reaction for extradiol cleavage.

catecholate, but not disodium catecholate, implying that catechol binds to the iron centre as the monoanion,⁵⁹ the same conclusion reached from EXAFS studies on the 2,3-CTD-catechol complex.⁶⁰

Studies of the mechanism of the FeCl_2 -TACN model reaction have shown that the role of pyridine is two-fold: one equivalent of pyridine is required as a base to generate catechol monoanion, but one equivalent of pyridinium chloride is subsequently required as a proton donor to assist the Criegee rearrangement for extradiol cleavage.⁵⁹ Cleavage in the presence of methanol, ethanol or isopropanol yields the respective various alkyl esters of 2-hydroxymuconic semialdehyde, implying the intermediacy of a 7-membered α -keto-lactone, as for the enzymatic reaction.⁵⁹ The close similarities of regioselectivity and substrate selectivity between this model reaction and the *E. coli* MhpB-catalysed enzymatic reaction suggest that they follow a similar mechanism.



Scheme 21 Axial/equatorial hypothesis for extradiol/intradiol dioxygenase selectivity.

In summary, model systems for extradiol cleavage have proved more elusive, but extradiol cleavage is observed for a tridentate macrocyclic ligand, complexed with Fe^{II} , which shows high selectivity and appears to follow the same mechanism as the enzyme-catalysed reaction. It is interesting to note that both Fe^{II} and Fe^{III} are capable of extradiol cleavage in this system, but that Fe^{II} shows higher rate and selectivity, providing some insight into why Fe^{II} is found as the cofactor in the extradiol dioxygenases. The two-fold role of pyridine in this model reaction also suggests a role for an active site base, and a proton donor, in the extradiol dioxygenase active sites. All of the extradiol dioxygenases which have been structurally elucidated have, as well as the iron(II) ligands, an additional histidine residue near to the substrate binding site, and a

tyrosine–histidine pair which could function as a proton donor (see Fig. 2).

A hypothesis for extradiol vs. intradiol selectivity

At this point the reader will see that the choice of intradiol vs. extradiol reaction pathway will be influenced strongly by the co-ordination chemistry of the metal centre, but that the choice of acyl vs. alkenyl migration which ultimately dictates the reaction products will also be influenced by stereoelectronic factors, notably the positioning of the hydroperoxide O–O bond. In this section we will present a hypothesis which may rationalise the selectivity shown by the extradiol and intradiol dioxygenases using a stereochemical model.

In Section 5 we reached the important conclusion that, although there is a different order of initial events in the intradiol vs. extradiol reaction mechanisms, the two reaction mechanisms converge on a common proximal hydroperoxide intermediate. The choice of intradiol vs. extradiol reaction pathways is then determined by acyl vs. alkenyl migration rearrangements of this hydroperoxide intermediate. In Section 6 we saw that there is chemical precedent for both acyl migration and alkenyl migration, but that the choice of migratory group may be governed by stereoelectronic factors. In Section 7 we saw that the co-ordination chemistry of the metal centre is also important for choice of reaction pathway: tetradentate iron(III) complexes are effective catalysts for intradiol cleavage, but that the more elusive extradiol cleavage reaction can be catalysed by a facial tridentate iron(II) complex. These co-ordination states mimic the situation observed in the respective dioxygenase active sites.

Our hypothesis to rationalise these observations is that there are two stable conformations for the proximal hydroperoxide intermediate: one in which the hydroperoxide group is situated in a pseudo-axial orientation, and one in which the hydroperoxide is situated in a pseudo-equatorial orientation. In the extradiol dioxygenase active site the His₂Glu motif provides three protein ligands for iron(II) (as found in the TACN model reaction). Assuming that the iron(II) centre can access an octahedral co-ordination geometry during the catalytic cycle,

then it is able to bind substrates and reaction intermediates *via* three co-ordination sites. It is therefore able to bind the proximal hydroperoxide intermediate in a tridentate fashion, and hence access the conformation in which hydroperoxide is pseudo-axial. In this conformation the hydroperoxide group is optimally aligned for alkenyl migration (*via* either σ bond migration or π participation) and hence undergoes extradiol cleavage.

In the intradiol dioxygenase active site the His₂Tyr₂ motif provides four protein ligands for iron(III) (as found in the tetradentate iron(III) models). Assuming that the iron(III) centre can access an octahedral co-ordination geometry during the catalytic cycle, then it is able to bind substrates and reaction intermediates *via* only two co-ordination sites. Bidentate co-ordination of the proximal hydroperoxide is not able to access the pseudo-axial hydroperoxide conformation, but instead binds as the pseudo-equatorial conformation, which then undergoes acyl migration. Why should an equatorial hydroperoxide promote acyl migration? One argument is that acyl migration is the 'default' option, as shown by the Baeyer–Villiger oxidation of 1,2-diketones. Alternatively, the axial hydroxy group is well positioned to attack the neighbouring ketone, which could initiate acyl migration *via* electrocyclic ring opening.³⁹

The weakness in this argument in the latter case is that the axial tyrosine ligand (Tyr-447) of 3,4-PCD has been shown to swing away from the iron(III) centre upon substrate binding, leaving only three protein ligands.¹⁷ However, presumably Tyr-447 is re-ligated to the iron(III) centre at the end of the catalytic cycle, so it is not clear whether it remains dissociated from the iron(III) centre throughout the reaction cycle, or becomes re-attached at some point. The observation that the majority of intradiol catalysts are tetradentate iron(III) complexes suggests that the availability of only two co-ordination sites may be a feature of the intradiol reaction.

Would this model explain the other amino acid sidechains found in the extradiol and intradiol active sites? Studies of the TACN extradiol model reaction imply a requirement for one base for substrate ligation, and one proton donor to assist alkenyl migration. In each of the extradiol active sites (see Fig. 2) there is a nearby histidine residue which could function as a base (His195 in BphC is situated 4.0 Å from the iron(II) centre),

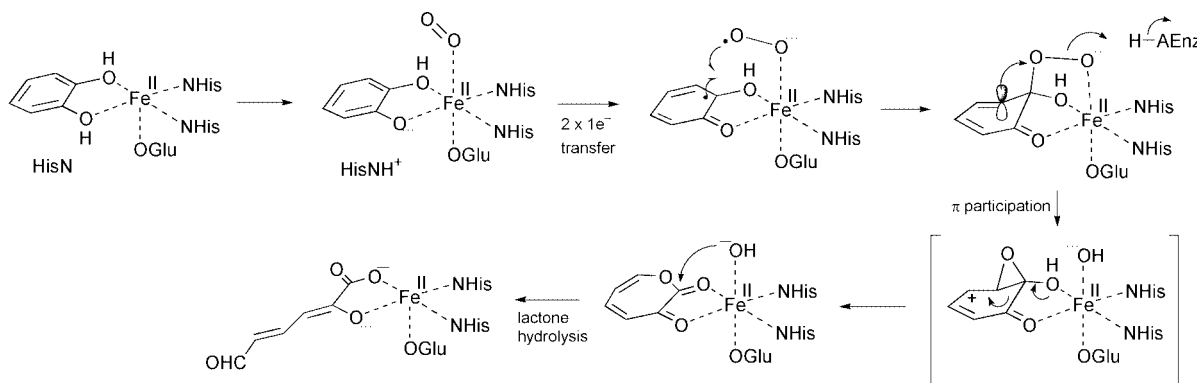


Fig. 6 Proposed catalytic mechanism for extradiol catechol cleavage, *via* an axial proximal hydroperoxide intermediate.

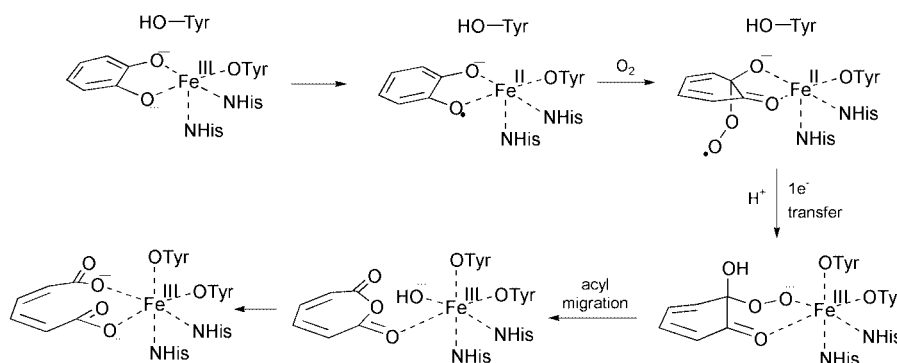


Fig. 7 Proposed catalytic mechanism for intradiol catechol cleavage, *via* an equatorial proximal hydroperoxide intermediate.

and also a nearby tyrosine–histidine pair which could function as a proton donor (Tyr250 in BphC is situated 3.8 Å from the iron(II) centre, with nearby His-241). The active sites of 3,4-PCD and 1,2-CTD (see Fig. 1) are, apart from the iron(III) ligands, notable for the absence of acid/base or polar amino acid sidechains, suggesting that the intradiol reaction requires relatively little catalytic assistance by the enzyme, consistent with the observation that a wide variety of tetradentate model systems are able to catalyse intradiol cleavage.

The overall catalytic mechanisms proposed for extradiol and intradiol cleavage are shown in Fig. 6 and 7. For extradiol cleavage, an active site base is required to generate the catechol mono-anion, and a proton donor is required to assist alkenyl migration. The iron(II) centre is able to activate both catechol and dioxygen, mediate one-electron transfers, assist alkenyl migration *via* Lewis acid catalysis, and activate Fe^{II}-hydroxide for lactone hydrolysis. For intradiol cleavage, substrate deprotonation appears to be driven by the stronger Lewis acidity of iron(III), which then activates the substrate for reaction with dioxygen, then mediates acyl migration, and assists hydrolysis of muconic anhydride. Both families of enzyme demonstrate the range of chemical functions carried out by non-haem iron in enzyme catalysis. A combination of mechanistic enzymology and small molecule model studies, in combination with protein crystallography, are now beginning to provide a rationalisation of how Nature has evolved two catalytic strategies for this difficult transformation, and the subtle chemical factors which control the choice of reaction pathway.

Acknowledgements

Studies in the author's laboratory have been supported by BBSRC and AstraZeneca Pharmaceuticals.

References

- 'Bioinorganic Enzymology', *Chem. Rev.*, whole issue (no. 7), 1996, **96**, 2237.
- For a previous review of the catechol dioxygenases see: T. D. H. Bugg and C. J. Winfield, *Nat. Prod. Rep.*, 1998, **15**, 513; L. Que, Jr. and R. Y. N. Ho, *Chem. Rev.*, 1996, **96**, 2607.
- S. Dagley, *Essays Biochem.*, 1975, **11**, 81.
- O. Hayaishi, M. Katagiri and S. Rothberg, *J. Am. Chem. Soc.*, 1955, **77**, 5450.
- Y. Kojima, N. Itada and O. Hayaishi, *J. Biol. Chem.*, 1961, **236**, 2223.
- O. Hayaishi, *Bacteriol. Rev.*, 1966, **30**, 720.
- D. H. Ohlendorf, J. D. Lipscomb and P. C. Weber, *Nature*, 1988, **336**, 403.
- D. H. Ohlendorf, A. M. Orville and J. D. Lipscomb, *J. Mol. Biol.*, 1994, **244**, 586.
- M. W. Vetting, C. A. Earhart and D. H. Ohlendorf, *J. Mol. Biol.*, 1994, **236**, 372.
- M. W. Vetting and D. H. Ohlendorf, *Structure*, 2000, **8**, 429.
- S. Han, L. D. Eltis, K. N. Timmis, S. W. Muchmore and J. T. Bolin, *Science*, 1995, **270**, 976.
- E. L. Hegg and L. Que, Jr., *Eur. J. Biochem.*, 1997, **250**, 625.
- T. Senda, S. Sugiyama, H. Narita, T. Yamamoto, K. Kimbara, M. Fukuda, M. Sato, K. Yano and Y. Mitsui, *J. Mol. Biol.*, 1996, **255**, 735.
- A. Kita, S. I. Kita, I. Fujisawa, K. Inaka, T. Ishida, K. Horiike, M. Nozaki and K. Miki, *Structure*, 1998, **7**, 25.
- K. Sugimoto, T. Senda, H. Aoshima, E. Masai, M. Fukuda and Y. Mitsui, *Structure*, 1999, **7**, 953.
- G. P. Titus, H. A. Mueller, J. Burgner, S. Rodriguez de Cordoba, M. A. Penalva and D. E. Timm, *Nature Struct. Biol.*, 2000, **7**, 542.
- A. M. Orville, J. D. Lipscomb and D. H. Ohlendorf, *Biochemistry*, 1997, **36**, 10 052.
- G. Hamilton, in *Molecular Mechanisms of Oxygen Activation*, ed. O. Hayaishi, Academic Press, New York, 1974, pp. 443–444.
- F. McCapra, *Acc. Chem. Res.*, 1976, **9**, 201; E. Conti, N. P. Franks and P. Brick, *Structure*, 1996, **4**, 287.
- T. H. Lowry and K. S. Richardson, in *Mechanism and Theory in Organic Chemistry*, Harper & Row, New York, 1976, pp. 327–332.
- For a comprehensive review of the Baeyer–Villiger oxidation see: G. R. Krow, *Org. React.*, 1993, **43**, 251.
- R. J. Mayer and L. Que, Jr., *J. Biol. Chem.*, 1984, **259**, 13056.
- J. Sanvoisin, G. J. Langley and T. D. H. Bugg, *J. Am. Chem. Soc.*, 1995, **117**, 7836.
- E. Lee-Ruff, *Chem. Soc. Rev.*, 1977, **6**, 195.
- C. Bianchini, P. Frediani, F. Laschi, A. Meli, F. Vizza and P. Zanello, *Inorg. Chem.*, 1990, **29**, 3402.
- P. Barbaro, C. Bianchini, C. Mealli and A. Meli, *J. Am. Chem. Soc.*, 1991, **113**, 3181.
- S. Dutta, S. M. Peng and S. Bhattacharya, *Inorg. Chem.*, 2000, **39**, 2231.
- R. Müller and F. Lingens, *Z. Naturforsch.*, 1989, **44c**, 207.
- J. W. Whittaker and J. D. Lipscomb, *J. Biol. Chem.*, 1984, **259**, 4476.
- J. W. Whittaker and J. D. Lipscomb, *J. Biol. Chem.*, 1984, **259**, 4487.
- D. M. Arciero and J. D. Lipscomb, *J. Biol. Chem.*, 1986, **261**, 2170.
- C. J. Suckling, *Angew. Chem., Intl. Ed. Engl.*, 1988, **27**, 537; D. C. Nonhebel, *Chem. Soc. Rev.*, 1993, **22**, 348.
- E. L. Spence, G. J. Langley and T. D. H. Bugg, *J. Am. Chem. Soc.*, 1996, **118**, 8336.
- D. D. Cox and L. Que, Jr., *J. Am. Chem. Soc.*, 1988, **110**, 8085.
- H. G. Jang, D. D. Cox and L. Que, Jr., *J. Am. Chem. Soc.*, 1991, **113**, 9200.
- C. J. Winfield, Z. Al-Mahrizy, M. Gravestock and T. D. H. Bugg, *J. Chem. Soc., Perkin Trans. 1*, 2000, 3277.
- P. M. Cullis, J. R. P. Arnold, M. Clarke, R. Howell, M. De Mira, M. Naylor and D. Nicholls, *J. Chem. Soc., Chem. Commun.*, 1987, 1088.
- M. F. Hawthorne and W. D. Emmons, *J. Am. Chem. Soc.*, 1958, **80**, 6398.
- K. L. Eley, P. J. Crowley and T. D. H. Bugg, *J. Org. Chem.*, 2001, **66**, 2091.
- R. M. Goodman and Y. Kishi, *J. Org. Chem.*, 1994, **59**, 5125; *J. Am. Chem. Soc.*, 1998, **120**, 9392.
- P. Deslongchamps, *Stereoelectronic Effects in Organic Chemistry*, Pergamon Press, Oxford, 1983, pp. 182–190.
- A. Nishinaga, K. Nakamura, T. Shimizu and T. Matsuura, *Tetrahedron Lett.*, 1979, 2165.
- E. J. Corey, W. G. Su and M. M. Mehrotra, *Tetrahedron Lett.*, 1984, **25**, 5123.
- E. J. Corey and M. M. Mehrotra, *Tetrahedron Lett.*, 1983, **24**, 4921.
- M. G. Weller and V. Weser, *J. Am. Chem. Soc.*, 1982, **104**, 1433.
- L. S. White, P. V. Nilsson, L. H. Pignolet and L. Que, Jr., *J. Am. Chem. Soc.*, 1984, **106**, 8312.
- L. Que, Jr., R. C. Kolanczyk and L. S. White, *J. Am. Chem. Soc.*, 1987, **109**, 5373.
- P. Mialane, L. Tchertanov, F. Banse, J. Sainton and J. J. Girerd, *Inorg. Chem.*, 2000, **39**, 2440.
- M. Duda, M. Pascaly and B. Krebs, *J. Chem. Soc., Chem. Commun.*, 1997, 835.
- R. Viswanathan, M. Palaniandavar, T. Balasubramanian and T. P. Muthiah, *Inorg. Chem.*, 1998, **37**, 2943.
- M. Pascaly, C. Nazikkol, F. Schweppe, A. Wiedemann, K. Zurlinden and B. Krebs, *Z. Anorg. Allg. Chem.*, 2000, **626**, 50.
- T. Funabiki, T. Yamazaki, A. Fukui, T. Tanaka and S. Yashida, *Angew. Chem., Intl. Ed. Engl.*, 1998, **37**, 4513.
- W. O. Koch and H. J. Kruger, *Angew. Chem., Intl. Ed. Engl.*, 1995, **34**, 2671.
- T. Funabiki, A. Mizoguchi, T. Sugimoto, S. Tada, M. Tsugi, H. Sakamoto and S. Yoshida, *J. Am. Chem. Soc.*, 1986, **108**, 2921.
- A. Dei, D. Gatteschi and L. Pardi, *Inorg. Chem.*, 1993, **32**, 1389.
- M. Ito and L. Que, Jr., *Angew. Chem., Intl. Ed. Engl.*, 1997, **36**, 1342.
- T. Ogihara, S. Hikichi, M. Akita and Y. Moro-oka, *Inorg. Chem.*, 1998, **37**, 2614.
- G. Lin, G. Reid and T. D. H. Bugg, *Chem. Commun.*, 2000, 1119.
- G. Lin, G. Reid and T. D. H. Bugg, *J. Am. Chem. Soc.*, 2001, in press.
- L. Shu, Y. M. Chiou, A. M. Orville, M. A. Miller, J. D. Lipscomb and L. Que, Jr., *Biochemistry*, 1995, **34**, 6649.